Available online at www.sciencedirect.com
ScienceDirect
International Journal of Pharmaceutics 343 (2007) 196–207
INTERNATIONAL JOURNAL OF PHARMACEUTICS
www.elsevier.com/locate/ijpharm

Modeling drug release from bioerodible microspheres using a cellular automaton

Nicolas Bertrand [1], Grégoire Leclair [2], Patrice Hildgen *

Faculty of Pharmacy, University of Montreal, C.P. 6128, succ. Centre-Ville, Montréal, Québec, Canada H3C 3J7

Received 13 October 2006; received in revised form 14 May 2007; accepted 15 May 2007
Available online 26 May 2007

Abstract

Mathematical modeling of drug release from biodegradable microspheres is designed to improve understanding of phenomena involved in this complex process. In spite of the considerable information obtained from conventional models, their use of equation curve fitting often limits the possibility to generalize their results. The objective of the presented study is to develop a model involving a three-dimensional cellular automaton to simulate both polymer erosion and drug diffusion independently. The model involves millions of independent cells in different states representing the components present in microspheres. The different states allow representation of polymer, drug, pores and solvent. For erosion, each cell is defined with a life expectancy and its chance of being eroded evolves according to the number of direct neighbours containing solvent. For diffusion, drug-containing cells are allowed to randomly diffuse their content in their neighbouring solvent-containing cells. Good correlations are obtained between simulations and two sets of experimental data obtained from release study at different pH. The model offers some insights about important drug release phases, like burst and subsequent release. Graphical representations obtained from the cellular automaton are also compared to SEM images. Cellular automaton proves to be an interesting tool for drug release modeling offering insights on the phenomena involved.

Keywords: Microspheres; Cellular automaton; Diffusion; Erosion; Drug release modeling; Monte Carlo modeling

1. Introduction

Since the introduction of microspheres (MS) as pharmaceutical drug releasing devices, numerous mathematical models have been proposed to simulate and elucidate the mechanisms involved in their behaviour (Batycky et al., 1997; Faisant et al., 2002, 2003; Lemaire et al., 2003; Siepmann et al., 2002; Tzafriri, 2000; Wada et al., 1995). Usually, these models focus on a few specific aspects controlling the drug release rates. For example, diffusion-controlled models are coupled in some way with polymer erosion in order to fit experimental results (Faisant et al., 2003; Lemaire et al., 2003; Siepmann et al., 2002; Wada et al., 1995). Although these methods give good understanding of a number of aspects involved in drug release, their versatility is often limited by the mathematical assumptions used to design them. Moreover, because they often regroup different considerations in a limited number of variables, the real importance of each mechanism remains hard to assess.

The purpose of this article is to use a cellular automaton to model independently the different phenomena involved in drug release. By adequately representing a MS in its environment, this will allow to address each mechanism separately and examine what role each of them plays in various phases of drug release.

The principles of cellular automaton were introduced by Von Neumann (1966). In these modeling tools, space is divided into a number of independent cells whose state evolves with time, according to information given by their neighbouring cells. After being used in various domains, cellular automata have been introduced in drug delivery to model drug release from bioerodible devices (Zygourakis and Markenscoff, 1996). From there, Monte Carlo models have evolved, becoming useful tools for erosion simulations (Göpferich, 1996; Göpferich and Langer, 1993, 1995a; Siepmann et al., 2002; Siepmann and Göpferich, 2001).

* Corresponding author. Tel.: +1 514 343 6448; fax: +1 514 343 6871.
E-mail addresses: nicolas.bertrand@umontreal.ca (N. Bertrand), patrice.hildgen@umontreal.ca (P. Hildgen).
[1] Tel.: +1 514 343 6111x0397; fax: +1 514 343 6871.
[2] Present address: Merck Frosst Canada & Co., 16711 Trans Canada Highway, Kirkland, Quebec, Canada H9H 3L1.

0378-5173/$ – see front matter © 2007 Elsevier B.V. All rights reserved.
doi:10.1016/j.ijpharm.2007.05.050

Indeed, because erosion is often critical in drug release from biodegradable polymeric matrices, it figures among the physical phenomena most frequently studied in models. Erosion is a complex phenomenon described as weight loss from polymer bulk (Göpferich, 1996, 1997). As it occurs from an intricate mass of entangled polymer chains, it is more complex than mere degradation (Larobina et al., 2002). Hence, for most polymers, erosion is known to occur in three steps (Larobina et al., 2002). First, solvent penetrates into the polymeric matrix (step 1). This step plays an important role in bulk erosion while being more marginal in surface eroding polymers (Von Burkersroda et al., 2002). After solvent ingress, chemical degradation of the "wetted" polymer occurs (step 2). The speed of hydrolysis is controlled by the nature of bonds and polymer structure as well as solvent conditions (pH and temperature, for example) (Göpferich, 1996). Finally, it is only with solubilisation and diffusion of oligomers out of the matrix (step 3) that real mass loss takes place. Unless the initial matrix contains an important number of short soluble chains, the third step is restricted by previous chemical degradation, occurring during step 2 (Batycky et al., 1997; Göpferich, 1997). Further bulk loss can be enhanced by detachment of small insoluble parts (Göpferich, 1997) as cohesion forces in the device are progressively reduced.

Another important phenomenon involved in drug release from polymeric MS is drug diffusion. In common mathematical models, the phenomenon is usually described by solving Fick's second law, a partial differential equation, either numerically (Lemaire et al., 2003; Siepmann et al., 2002) or by estimation with simpler equations (Wada et al., 1995; Faisant et al., 2002). For biodegradable polymeric matrices, these methods offer good fitting of experimental data when the diffusion coefficient is accounted to vary with time (Batycky et al., 1997; Faisant et al., 2002, 2003; Siepmann et al., 2002; Wada et al., 1995). However, as diffusion is highly influenced by the environment (Higuchi, 1963), the single diffusion coefficient obtained from these models offers little information on drug and/or pore configuration or drug–polymer interactions. To circumvent this, diffusion is presented here as a self-governing mechanism: basic Brownian motion of the drug in its environment.

Therefore, the three-dimensional model presented in this article must be viewed as a way to offer new means of understanding MS behaviour instead of as a replacement of already proven mathematical models. Here, two important aspects of drug release are studied simultaneously yet independently; erosion by a model inspired from Zygourakis' work and diffusion by simulated molecular movement of drug through the matrix. To examine the accuracy and limitations of the model, simulations were compared with two sets of experimental data obtained from a batch of ibuprofen-containing MS. The two release studies were conducted under different conditions, namely at alkaline pH (where polymer degradation occurs rapidly) and at neutral pH (where polymer degradation is slow). Although good fitting with experimental curves and increased comprehension of drug release mechanisms were expected, it was also anticipated that differences between erosion kinetics in the two experiments would emphasize certain model inadequacies that should be addressed in the future.

2. Materials and methods

2.1. DL-PLA synthesis

The DL-polylactide polymer was synthesized according to a modified method described earlier (Nadeau and Hildgen, 2005). The DL-dilactide (100 g, 694 mmol) and tetraphenyltin (29 mg, 0.068 mmol) were dissolved in toluene and dried by rotary evaporation to remove water from the reaction mixture. The reaction was conducted under argon atmosphere at 180 °C for 3.3 h. The mixture was cooled to ambient temperature before being dissolved in acetone and precipitated in water. The polymer was washed and dried under vacuum to yield 85 g (85%) of white polymer.

2.2. Microsphere preparation

Several batches of MS were prepared using a modified solvent-evaporation method published earlier (Panoyan et al., 2003). Polymer (3.75 g) and ibuprofen (375 mg) were dissolved in 50 mL dichloromethane and emulsified in 4 L of 0.5% PVA solution by continuous circulation through a sonication chamber (550 Sonic Dismembrator, Fisher Scientific, USA). The speed of injection of the drug/polymer solution into the sonication chamber and flow of PVA solution through the chamber were set, respectively, to 290 mL/h and 350–400 mL/min. The sonication intensity was set to 20% and stopped after the complete injection of the dichloromethane phase. After emulsification, dichloromethane was evaporated under reduced pressure and constant stirring for at least 4 h. MS were washed twice with water, collected by centrifugation at 20,000 × *g* and lyophilized prior to storage.

2.3. MS characterization: particle size analysis, drug loading, density and porosimetry

Five batches of MS were prepared using the method described above; the particles were sieved through a 325 mesh USP sieve (Fisher Scientific, USA) and pooled into a single 8 g batch. The particle size of the lot was measured by differential light scattering using a Coulter LS 230 Particle Size Analyzer (Beckman Coulter, USA). MS were suspended in water (>8% obscuration) using the small volume module and the PIDS option. The measurements were conducted at room temperature in quadruplicate.

Drug loading was determined by digestion of approximately 20 mg of precisely weighed particles in 6 mL of 1N NaOH. Ibuprofen concentration was measured by spectrophotometry (Hitachi U-2001, Japan) at 264 and 272 nm to detect eventual interference of degraded polymer. This experiment was done in triplicate.

MS density was measured with a helium Ultrapycnometer 1000 (Quantachrome Instruments, USA) at room temperature (23 °C) and 19 psi, in the precalibrated small experimentation cell. The results of 10 measurements were averaged.

Porosity measurements were conducted by nitrogen adsorption at 77 K with an Autosorb-1^{TM} instrument (Quantachrome

Instruments, USA). Particles were weighed, outgassed for 12 h and analyzed for a five-point BET involving 20 absorption and 20 desorption points. Total pore volume was evaluated from the total pore distribution obtained with the Dollimore and Heal method on desorption points (Dollimore, 1964; Dollimore and Heal, 1970).

2.4. Release study

Release studies were conducted in two different phosphate buffers (study A at pH 11.9 and study B at pH 7.4). About 100 mg of MS were precisely weighed and placed in a dialysis bag (SpectraPor 1, *cut-off* of 6–8000 Da, Spectra, USA). Particles were suspended in a small amount of buffer, before closure of the bag. The bags were placed in 20 mL of buffer solution (total quantity, with buffer volume in the bag) in tubes. Five-millilitre aliquots were withdrawn at each time point and replaced with fresh buffer. The release study was conducted in triplicates on a vertical rotating plate at 37 °C for 2 weeks in the alkaline buffer and for 22 weeks in the neutral buffer. In the latter case, to ascertain the amount of residual drug in the particle, remains of one sample was fully digested by addition of 10 mL of 2N sodium hydroxide solution. The remaining two samples were kept for SEM imaging and further analysis.

Drug diffusion through the dialysis bag was not rate-limiting as release from a saturated ibuprofen solution was much more rapid than its release from the MS, in both buffers (data not shown). Furthermore, although drug solubility was different in each medium (∼50 mg/mL at pH 7.4 and ∼337 mg/mL at pH 11.9 (Higgins et al., 2001)), the low drug loading of particles and the high volume of medium used (above 20 mL) ensured sink conditions throughout study, while the low pK_a of ibuprofen (4.5–4.6 (Higgins et al., 2001)) assured extensive ionization at both pH values studied. Likewise, it was proven that, for low drug concentrations (Van Drooge et al., 2006), drug in polymeric matrices is dispersed as a solid solution (Liggins and Burt, 2004; Lin et al., 1999; Cui et al., 2003; Vachon and Nairn, 1995; Klose et al., 2006). For this reason, and because absence of crystalline ibuprofen was confirmed experimentally by the lack of drug melting point at 75 °C on DSC spectra (data not shown), drug dissolution is not expected to be a limiting factor (Williams et al., 2005; Messaritaki et al., 2005; Klose et al., 2006).

2.5. Molecular weight analysis, scanning electron microscopy and differential scanning calorimetry

In order not to interfere with the main release studies, the following characterization was performed on samples recovered from parallel release studies, conducted as presented earlier and aborted at each time point. Dialysis bags were opened; particles recovered and lyophilized until further use.

Polymer molecular weight was measured by gel permeation chromatography on a Water associate system with a differential refractometer 2410 and three Styragel columns (HR3, HR4, HR6) (Waters, USA). Tetrahydrofuran was used as mobile phase at a flow rate of 1 mL/min, at 35 °C. Polystyrene standards were used for a 10-point calibration.

Scanning electron microscopy (SEM) images were obtained on a JSM-5900LV Scanning Electron Microscope (JEOL, Japan), in low vacuum mode (18–20 Pa), at 15 kV. Since environmental mode was used for image acquisition, particles were imaged as obtained, without coating.

Differential scanning calorimetry was performed on a TA instruments DSC Q1000 model (TA Instruments, USA). Samples were precisely weighed in aluminium pans and scanned from −20 to 100 °C at a heating and cooling rate of 10 °C/min.

3. Cellular automaton conception

The program was written in the C computing language on a Linux Red Hat 9.0 OS running on a Pentium IV 2.4 GHz and 1024 Mb of DDR RAM. The graphical representations were obtained using the POV-Ray 3.6 program (available online at www.povray.org) A list of abbreviations and symbols is presented in Table 1.

The cellular automaton is based on a virtual matrix defined in a cubic space of side $d = 200$ (8 million cells) and five states are

Table 1
List of abbreviations and symbols used in text

MS	Microspheres
d	Dimension of the virtual cubic matrix
S	Solvent state
P	Polymer state
E	Porosity state
D	Drug state
SD	Solubilised drug state
i, j, and k	Spatial coordinates in the matrix
P_{ijk}	Non-erosion probability of a specific cell in the matrix
Π_c	Intrinsic non-erosion probability of a specific compound
n	Number of neighbours of state S (containing solvent)
I_c	Discrepancy index between observations and simulations
E_t	Experimental observation at time t
S_t	Simulated result at time t
N	Number of time-points used for a specific discrepancy index calculation
I_{SD}	Discrepancy index between an all-SD sphere and a numerical solution of Fick's second law
I_{SimI}	Discrepancy index between study A and simulation I (whole study)
$I_{SimI(t<24\,h)}$	Discrepancy index between study A and simulation I (first 24 h)
$I_{A\text{-}N/E}$	Discrepancy index between study A and simulation N/E (first 24 h)
I_{SimIIa}	Discrepancy index between study B and simulation IIa (whole study)
$I_{SimIIa(t<504\,h)}$	Discrepancy index between study B and simulation IIa (first 504 h)
$I_{SimIIa(t>504\,h)}$	Discrepancy index between study B and simulation IIa (after 504 h)
I_{SimIIb}	Discrepancy index between study B and simulation IIb (whole study)
$I_{SimIIb(t<24\,h)}$	Discrepancy index between study B and simulation IIb (first 24 h)
$I_{B\text{-}N/E}$	Discrepancy index between study B and simulation N/E (first 24 h)

possible for each cell. Each state represents different physical components existing during drug release; polymer (P), solvent (S), porosity (E), solid drug (D) or drug in its solubilised form (SD). Throughout the simulation, the matrix follows successive iterations during which the state of each cell evolves. After one iteration, the number of cells in each state is counted; kinetics of drug release can be followed with the amount of drug cells remaining in the matrix.

3.1. P, polymer state

The P state represents the frame of the virtual MS. Its shape is defined as the largest spherical form possible in a virtual space of size d. Thus, state P is temporarily attributed to all cells (i; j; k) according to the equation:

$$i^2 + j^2 + k^2 \leq \left(\frac{d}{2}\right)^2 \quad (1)$$

In the present automaton as in other models (Göpferich, 1996, 1997; Siepmann et al., 2002; Zygourakis and Markenscoff, 1996), steps 2 and 3 of polymer erosion are combined in one single event. Thus, each P cell is attributed a life expectancy. A cell's life expectancy represents its resistance to erosion; the higher this parameter, the longer it will take before the cell gets eroded.

To insure heterogeneous erosion (Göpferich, 1996; Faisant et al., 2003; Göpferich and Langer, 1993, 1995b; Siepmann et al., 2002; Zygourakis and Markenscoff, 1996), a continuous distribution of intrinsic life expectancy (Π_{Px}) is calculated for different categories of P cells. All polymer categories are then randomly distributed through the matrix according to a normal distribution.

At each iteration during simulation, P cells undergo one non-erosion test against its non-erosion probability (P_{ijk}). The later is defined by Eq. (2) according to the intrinsic life expectancy of the cell (Π_c) and its number of neighbours in the S state (n).

$$P_{ijk} = \left(1 - \frac{1}{\Pi_c}\right)^n \quad (2)$$

If this test succeeds, the cell (i; j; k) remains in the same state P; if it fails, the cell is deleted (eroded) and becomes of state S. The nature of Eq. (2) ensures that the test will always succeed if none of a cell's neighbours contain solvent ($P_{ijk} = 1$ if $n = 0$) and the highest chance of erosion will occur if its six neighbours contain solvent.

3.2. S, solvent state

The S state represents the MS surrounding medium where drug is released. S cells are initially distributed at the periphery of the polymeric matrix. These cells represent the sink conditions outside the MS. During simulation, the S state corresponds to the *quiescent* state of the cellular automaton (total equilibrium is reached when all cells are of S state) and play a passive role in polymer erosion and drug dissolution.

3.3. E, porosity state

The E state represents pores in the MS. During matrix conception, the user defines the percentage of porosity in the MS. Pores are distributed in the form of connecting tunnels, according to a self-avoiding random walk, throughout the polymer. During simulation, E cells are replaced with S cells as soon as at least one of their neighbours is in S state.

3.4. D, solid drug state

The D state represents drug molecules distributed throughout the polymeric matrix, in the form of a solid solution. During matrix conception, drug loading defines the percentage of cells occupied initially with randomly distributed D cells. During simulation, D cells are replaced with SD cells as soon as at least one of their neighbours is in S state.

3.5. SD, solubilised drug state

The SD state is not present during matrix conception as it is a result of drug dissolution. To allow for drug diffusion in the matrix, SD cells follow different rules. As diffusion occurs predominantly in solvent, all SD cells are allowed to move into one of their neighbouring cells of state S. This movement is randomly decided between neighbouring S cells, with equal chances for all. During one iteration, every SD cells undergoes 400 random movements. SD cells are considered to reach sink conditions around the MS when they reach spatial coordinates outside the initial sphere of radius $d/2$. At this time, SD cells become regular S cells. This remains realistic as it is expected that polymer erosion will undergo bulk erosion and that matrix integrity will be conserved until most of the drug has been released. Finally, it is noteworthy that the number of SD cells never exceeds solubility for the amount of solvent inside the MS (solubility values calculated for pH 7.4 and pH 11.9 in simulation I and II, respectively).

3.6. Representing discrepancy between simulations and experimental results

Evaluation of the model predictivity cannot be obtained by common goodness-of-fit tests because the cellular automaton intends to be a mechanistic model, and is not using any fitting algorithm. Consequently, a method previously described for physiological pharmacokinetic models was used (Kannan et al., 1995). This approach uses a weighted mean squared-difference between experimental observation (E_t) and simulation results (S_t) at time t, for a number of time-points (N). A discrepancy index (I_c) is thus calculated with Eq. (3):

$$I_c = \frac{\sqrt{\sum_{t=1}^{N}(E_t - S_t)^2/N}}{\sqrt{\sum_{t=1}^{N}(E_t)^2/N}} \quad (3)$$

This index provides relative error evaluation of the model between 0 and 1, with low values (<0.2) suggesting good descrip-

tion (Kannan et al., 1995). Moreover, because this index can be calculated for any number of experimental values, relative predictivity can be compared throughout a single simulation for different time intervals.

4. Results and discussion

Results of the MS characterization experiments are presented in Table 2. Since the main purpose of these experiments was to obtain simulation parameters for the model, important assumptions must be taken into consideration.

Firstly, the model uses one spherical representation for the modeling of an experiment which contains thousands of independent MS. Although MS particle size distribution seems somewhat bimodal (Fig. 1, $t = 0$ h), a non-linear regression was found to offer very good correlations with a lognormal distribution ($R^2 = 0.9876$), with mean, median and mode values within confidence intervals. Consequently, it was assumed that

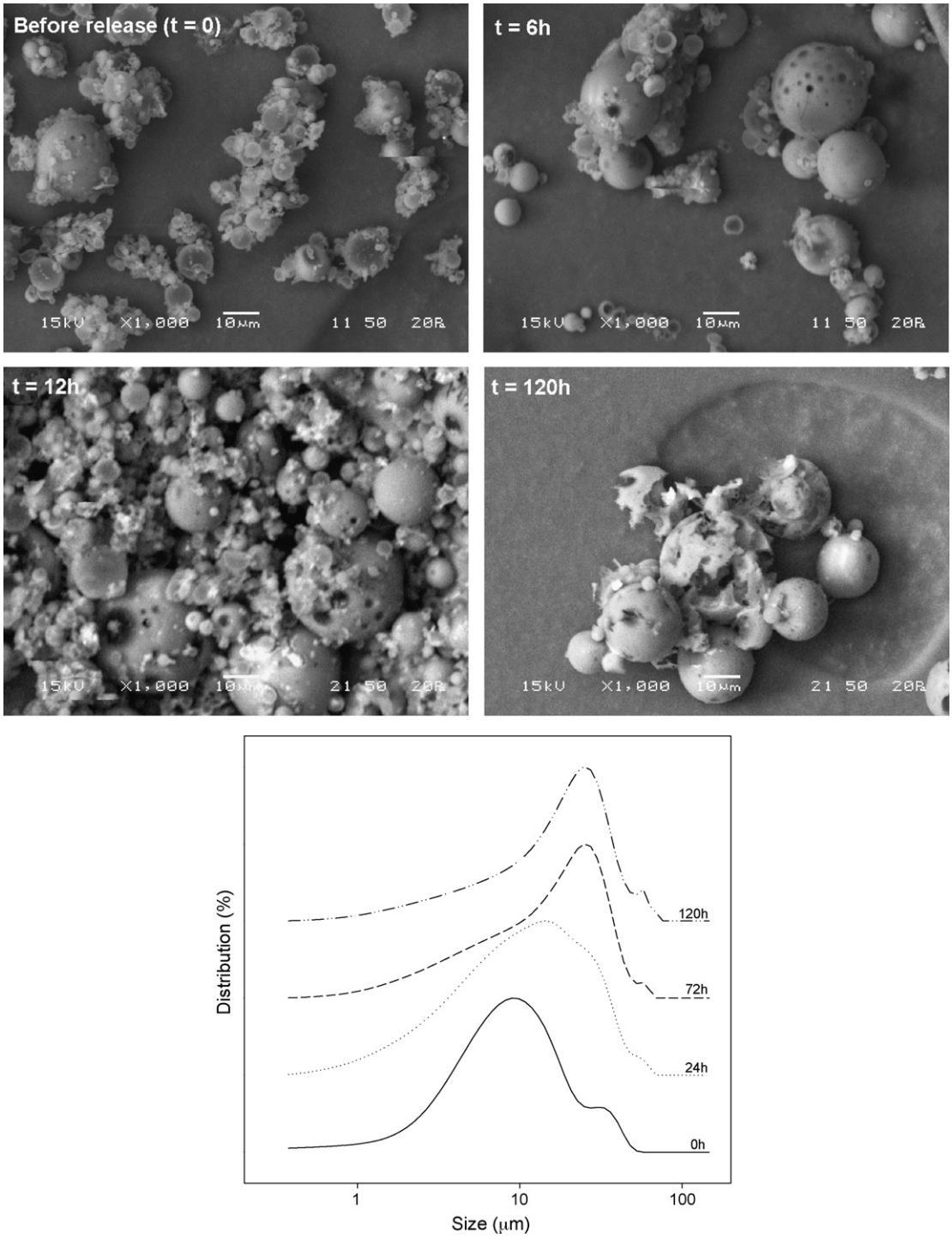

Fig. 1. SEM images of particles and particle size analysis taken at different time-points before and during release study A.

Table 2
Experimental particle characterization results

Polymer molecular weight before release study	
M_n	44,702 g/mol
M_w	66,106 g/mol
PI	1.4788
Differential light scattering ($n=4$)	
Mean size	8.09 μm ± 2.89
Median size	5.92 μm ± 0.1
Mode	6.58 μm ± 0.25
S.D.	7.33
<90%	17.16 μm
Drug loading ($n=3$)	6.28% (w/w) ± 0.34
True density ($n=10$)	1.35 g/cm^3
Porosity ($n=1$)	
Specific pore volume	0.021 cm^3/g

Same batch used for both release studies.

the sphere described in the model symbolizes an *average particle* that represents a specific lot of MS as a whole. As all MS are formulated using the same method, it is expected that they have the same properties and that the *average particle* offers a good representation of all particles. Although simplistic, this modeling hypothesis is similar to others where unique parameters, like diffusion coefficients, are fitted over the release kinetics of distributions of particles (Lemaire et al., 2003; Siepmann et al., 2002, 2004; Tzafriri, 2000; Wada et al., 1995; Faisant et al., 2002, 2003).

Secondly, it is noteworthy to mention that the raw data acquired during characterization was not used as obtained since the virtual sphere represented in the model is a weightless volume. As a result, drug loading and porosity had to be calculated with respect to the sphere volume. Moreover, in accordance with the drug solid solution hypothesis, total drug volume (5%) was calculated from the summation of all (6.28%, w/w) individual ibuprofen molecules volume (calculated with the Chem3D program; CambridgeSoft Corporation, USA). Similarly, total porosity (10%) was approximated from gas adsorption porosity measurements, which only represent pores in contact with the exterior of the MS.

Two different release studies were conducted simultaneously in the same conditions at pH 11.9 (study A) and pH 7.4 (study B). Although release pH of study A is radically non-physiological, different release conditions were used on the same MS batch in order to insure that erosion conditions were different between both experiments. Accordingly, differences between simulations revolved around polymer life expectancy, and will be discussed in more detail further. Experimental and simulated results are presented in Figs. 2A and 5A (study A versus *simulation I* and study B versus *simulation IIa/IIb*, respectively). Parameters used in each simulation are described in Table 3.

Lastly, to represent experiments and simulations on the same time axis, a conversion scale of 1 h for each 100 iterations was used. With this time scale and 400 movements per iteration, the calculated effective diffusion coefficient for SD was 2.95×10^{-11} cm^2/s, a value comparable to the one found in literature for similar systems (Faisant et al., 2002, 2003; Lemaire et al., 2003; Wada et al., 1995; Messaritaki et al., 2005). This fitting of time scales allowed perfect reproducibility for different simulation reruns, the large number of cells and iterations minimizing the importance of individual random events. It is noteworthy that the aptitude of the random walk model to represent diffusion was confirmed by the almost perfect fit ($I_{SD}=0.008$) of an all-SD matrix simulation over the numerical solution for Fick's second law, for a sphere with constant concentration at the surface (data not shown).

4.1. Study A (pH 11.9)

Drug release in study A was found to be rapid and complete (>85%) after 2 weeks. In this study, aggressive conditions led to extensive polymer degradation and to rapid matrix erosion while ensuring high drug accessibility for solvent. Hence, the drug does not remain trapped in the polymer and can freely diffuse out of the polymer bulk. Comparison of cellular automaton *simulation I* with release study A (Fig. 2A) shows very good fit ($I_{SimI}=0.054$) throughout the experiment and validates the ability of the model to simulate drug release from eroding particles. This tends to confirm that the combination of steps 2 and 3 of the erosion process in a single probability allows, in this case, good depiction of polymer erosion.

In this experimental study, alkaline conditions led to almost complete erosion because of rapid degradation of the polymer chains. The bulk erosion known to occur for PLA (Von Burkersroda et al., 2002) is also confirmed by experimental results obtained from this study. Particle erosion primarily

Table 3
Simulation parameters

	Simulation I	Simulation IIa	Simulation IIb	Simulation N/E[a]
General				
Diameter of matrix	200	200	200	200
Drug loading	4.5%	4.5%	4.5%	4.5%
Porosity	10%	10%	10%	10%
Drug life expectancy	1	1	1	1
Polymer				
Mean life expectancy	1,000,000	5,000,000	5,000,000	∞[a]
Minimum life expectancy	10	5000	5000	∞[a]
Life expectancy distribution	Log normal	Log normal	Modified[a]	N/A

[a] See text.

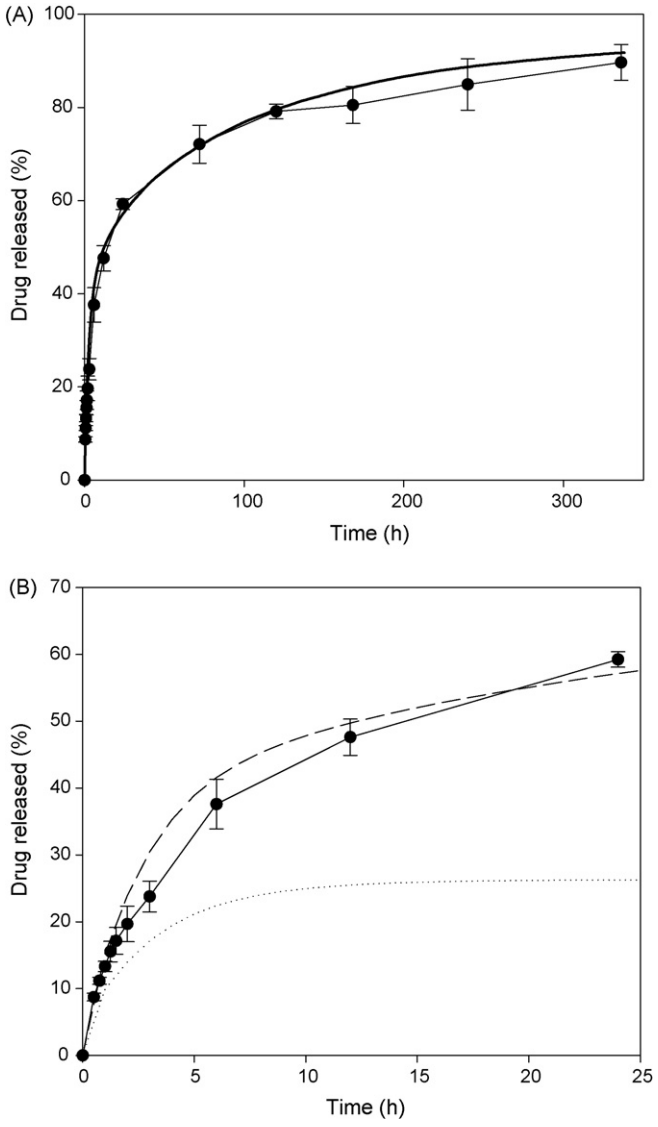

Fig. 2. Release study A, at 37 °C and pH 11.9. (A) Total experimental period (experimental results (●), *simulation I* (solid line)). (B) First 24 h of release (experimental results (●), *simulation I* (dashed line), *simulation N/E* (doted line)).

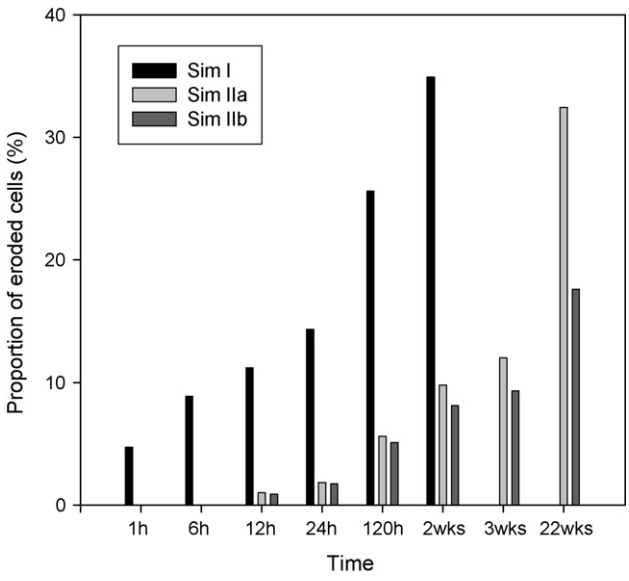

Fig. 3. Proportion of polymer cells eroded at different time-points in each simulation.

occurred by the widening already existing pores until they coalescence, causing complete destruction of the particle. Images shown in Fig. 1 display particles increasingly dimpled with time, while particle size analysis reveals disappearance of small particles. Both these observations show that bulk erosion leads to rapid destruction of smaller particles. Moreover, GPC studies conducted after 1 week showed decreased molecular weights ($M_n = 11{,}754$; $M_w = 21{,}139$, PI = 1.80) while loss of sphericity was observable by SEM, after 5 days (Fig. 1, $t = 120$ h).

On the cellular automaton simulation side, the life expectancy distribution of polymer cells was optimized to insure accurate drug release. Hence, Fig. 3 shows the amount of polymer cells eroded at significant time-points. For *simulation I*, the limited proportion of cells eroded during the first hours of drug release is consistent with bulk erosion theory, and SEM observations showing that particles maintained their shape. Accordingly, this shows again that model simplifications in erosion description seem to offer correct representation

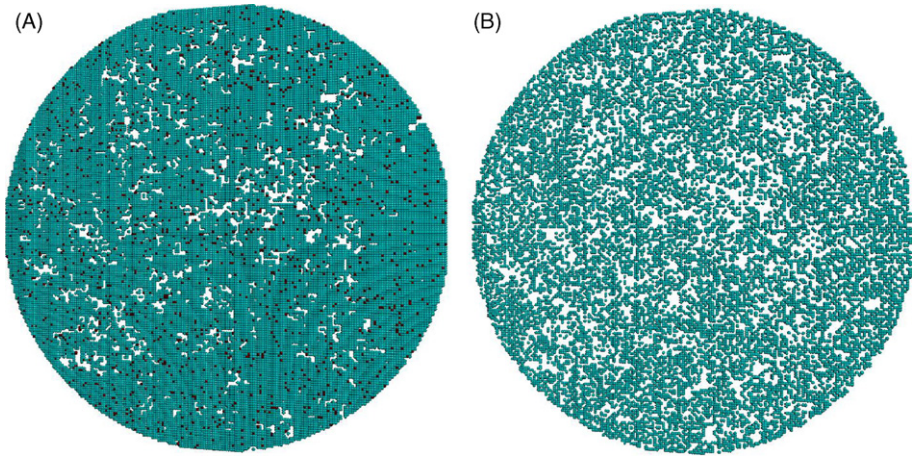

Fig. 4. Graphical representation of a longitudinal cut of the matrix at the beginning (A) and at the end (B) of simulation I. Increased porosity can be observed as a result of bulk erosion.

of experimental polymer erosion when degradation occurs rapidly.

However, for later time-points, comparisons of graphical representations of the matrix after simulation (Fig. 4) with SEM images after 120 h (Fig. 1) tend to show that erosion in the model is not as extensive as observed experimentally. This inaccuracy can be explained by the fact that the model does not take into account the detachment of solid non-eroded parts that are set free from the MS when pores coalesce. Although it is difficult to determine the amount of polymer that separates from the particles this way, images shown in Fig. 1 ($t = 24$ h and $t = 120$ h) clearly illustrate rough edges that could arise from detachment of solid parts. It remains unclear if this attrition occurred during drug release or during sample preparation prior to SEM analysis (involving filtration and freeze drying). Nevertheless, this discrepancy between simulated and experimental particle morphology does not seem to have much influence on drug release kinetics.

Finally, Fig. 2B emphasizes the first 24 h during which ~60% of the drug is released. Again on this time scale, good comparison ($I_{\mathrm{SimI}(t<24\,\mathrm{h})} = 0.104$) is achieved between experimental results and *simulation I* where, as shown in Fig. 3, around 15% of polymer cells are eroded. To assess the role of erosion during this first phase of release, another simulation was run with the matrix used in *simulation I* but without allowing polymer cells to erode (*simulation N/E*).

As expected, a clear difference in drug release is visible between simulations throughout the whole time period. *Simulation N/E* rapidly reaches a maximum amount of drug released (~26%). As the polymer matrix remains unchanged in this simulation, this limit corresponds to drug which is initially accessible to solvent. Consequently, differences between *simulation N/E* and experimental drug release ($I_{\mathrm{A\text{-}N/E}} = 0.478$) tend to show that, for this specific fast degrading system, erosion plays a role even in the early stages of drug release. Indeed, because degradation is fast, polymer chains rapidly reach a length for which their dissolution and diffusion out of the matrix is possible. The eroding polymer makes drug more accessible to penetrating solvent and larger quantities are allowed to diffuse out of the MS. Consequently for these MS in these precise conditions, fast degradation insures extensive and rapid release, during the first hours.

4.2. Study B (pH 7.4)

As expected, drug release at pH 7.4 is slower (Fig. 5A) than at alkaline pH. Indeed, study B lasts for 22 complete weeks (11 times the length of study A) and drug release is limited to less than 60% of the total drug content (terminal MS digestion led to recovery of 96% of initial drug loading). After an initial burst, the drug release rate decreases over a few weeks until it reaches a plateau. In mild conditions, this incomplete drug release from high molecular weight PLA MS was reported earlier (Liggins and Burt, 2001, 2004). Thus, as expected, surrounding conditions highly influence drug release rates from MS, presumably because of different erosion kinetics.

Indeed, it is known that, for high molecular weight PLA in mild conditions (such as the neutral pH used in study B), erosion

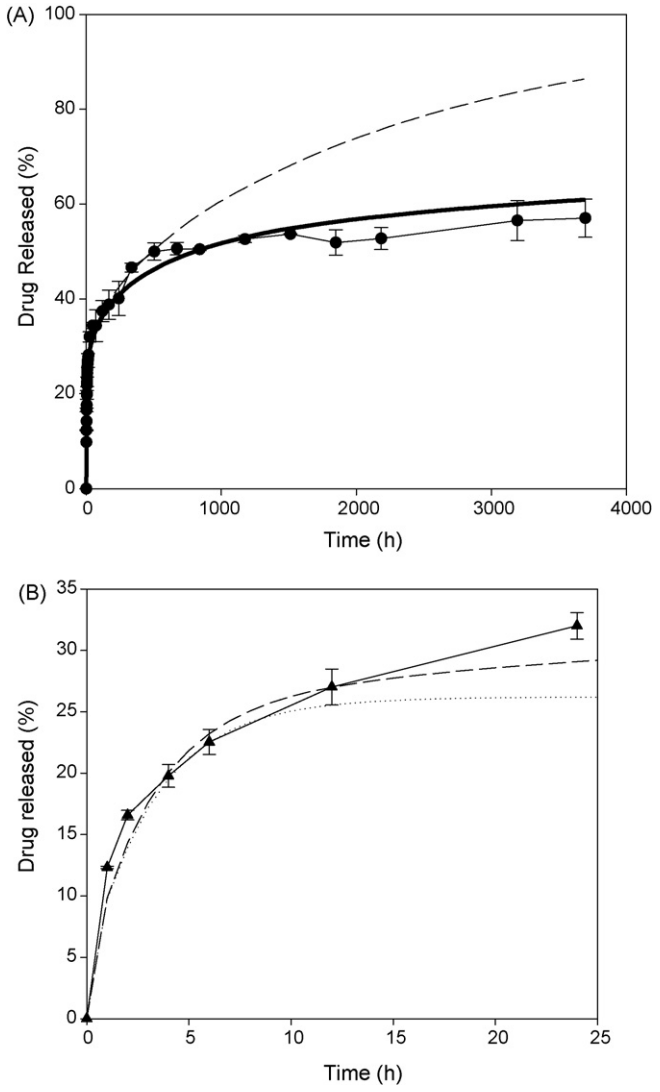

Fig. 5. Release study B, at 37 °C and pH 7.4. (A) Total experimental period (experimental results (●), *simulation IIa* (dashed line), *simulation IIb* (solid line)). (B) First 24 h of release (experimental results (▲), *simulation IIb* (dashed line), *simulation N/E* (doted line)).

occurs in a two-step process, at relatively high rates in the first hours with a drastic slowdown afterwards (Delgado et al., 1996; Park, 1994; Blanco et al., 2006) When degradation is slow, the first step is due to the departure of shorter, more mobile, polymer chains (Park, 1994; Dunne et al., 2000). This phenomenon seems enhanced for MS prepared by sonication (Blanco et al., 2006). Once these chains are depleted, long polymer chains remain extensively present in the bulk, enhancing its cohesion and decreasing its total mass loss, thus slowing erosion. Further erosion is possible solely when degradation has considerably decreased bulk cohesion and allowed short polymer chains to leave the matrix (Park, 1994).

Correspondingly, SEM images taken after 22 weeks (Fig. 6) show reduced erosion in study B compared to study A (Fig. 1). Moreover, coexistence of smooth-surfaced (non-eroded) and dimpled particles prove that erosion occurs, but in a less extensive manner than what was observed in study A. Likewise, GPC

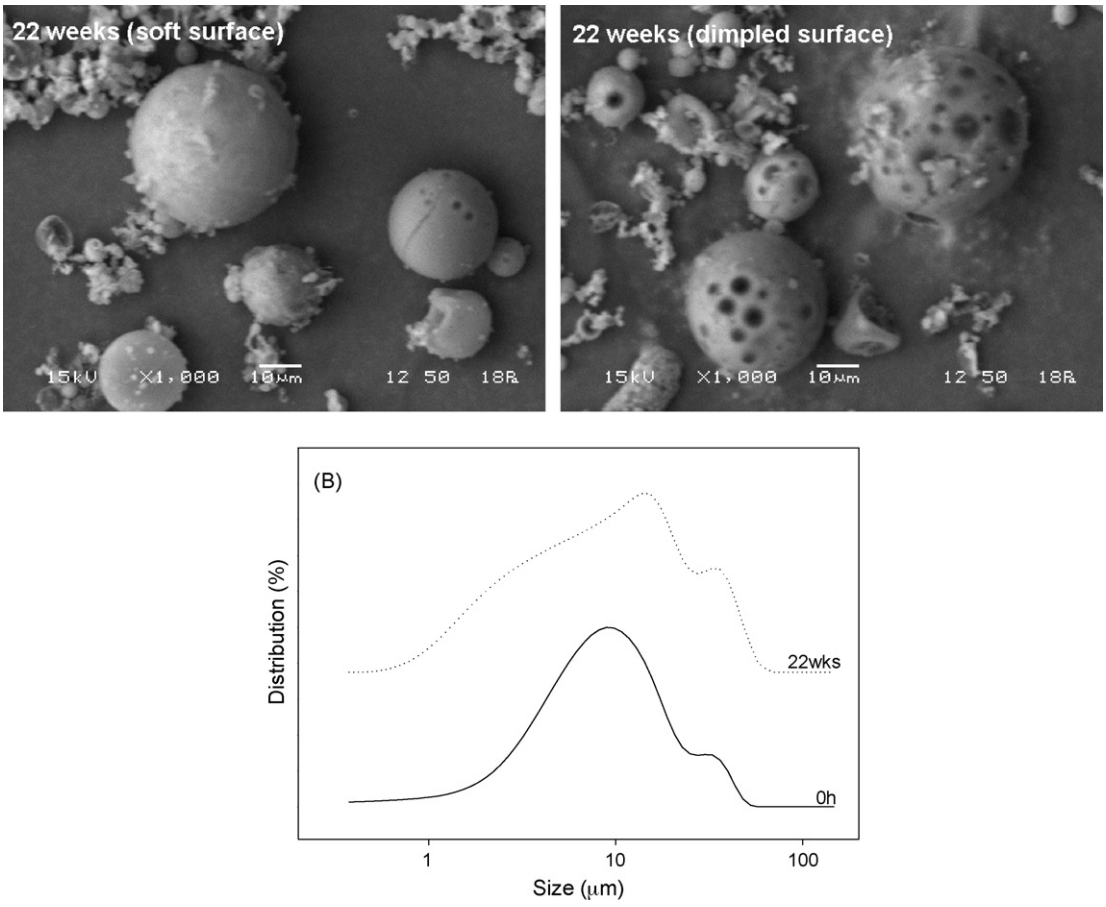

Fig. 6. SEM images of particles and particle size analysis at the end of study B (after 22 weeks).

studies at the end of release study B showed signs of degradation with decreased molecular weights (M_n = 15,424; M_w = 30,538) while high polydispersity index (PI = 1.9794) indicated the coexistence of low and high molecular weight polymer chains trapped in the bulk.

Conclusively, particle size analysis after 22 weeks (Fig. 6) shows a broad distribution comparable to the initial one, where even smaller, easily disappearing particles maintain their structure when exposed to mild conditions. This reinforces the notion of enhanced particle cohesion throughout the study, further proving that polymer erosion and bulk mass loss were present yet less extensive during study B.

In the simulation, this two-step erosion process differs from the assumptions previously used. The consequences of these dissimilarities can be observed in Fig. 5A where *simulation IIa* is compared to experimental results (I_{SimIIa} = 0.282). Although, the first 3 weeks (504 h) of drug release seem rather realistically depicted ($I_{SimIIa(t < 504\,h)}$ = 0.048), it is clear that correlations between *simulation IIa* and experiments greatly decrease afterward ($I_{SimIIa(t > 504\,h)}$ = 0.381). This initial period is thought to represent the first phase of polymer erosion, where short and medium chains are slowly driven out of the matrix. Around 12% of polymer cells are eroded in the simulation during this time (Fig. 3). However, after that phase, while experimental drug release essentially stops as a consequence of the decrease in erosion rate, *simulation IIa* never reaches this plateau.

It therefore seems that, in these experimental conditions, the continuous distribution of life expectancies in the model is not able to properly represent erosion. Indeed, in the mild conditions of study B, slower degradation leads to a depletion of small polymer chains. Hence afterwards, erosion becomes controlled by an all-or-nothing phenomenon where chains are either small enough to diffuse out or not. Unlike in study A where fast degradation ensures a uniform rate of erosion (easily represented with a simple probability test), study B shows different rates for steps 2 and 3, combined in the simulated erosion event. This makes simulations unable to illustrate the changes in erosion rate that are seen experimentally.

Therefore, *simulation IIb* was used to better portray drug release in study B. In this simulation, the continuity of the polymer life expectancy distribution is disrupted. Thus, Π_{Px} is augmented for a part of the polymer categories, making a majority of cells 10^6 times less likely to erode, while leaving other polymer cells unchanged. This modification led to separation of cells in easily erodible and almost non-erodible polymer, allowing drug release rate to decrease radically once easily-eroding cells were depleted. Fig. 3 shows differences between *simulation IIa* and *IIb* in the number of cells eroded at different time-points, while Fig. 5A shows a much better fitting (I_{SimIIb} = 0.059) of *simulations IIb* over the experimental release. It is thus evident that erosion is the main factor controlling drug release, especially in the later phase.

In order to better understand the role of erosion in study B, special attention was brought to the first 24 h of drug release. Fig. 5B presents the relatively good fitting of *simulation IIb* during this time period ($I_{\mathrm{SimIIb}(t<24\,\mathrm{h})} = 0.082$). Once again, the experimental drug release was compared to a simulation where polymer erosion was not possible (*simulation N/E*). Although this simulation was seen to differ greatly from reality in previous study A, it is interesting to note that it better depicts drug release in study B ($I_{\mathrm{B\text{-}N/E}} = 0.126$). Indeed, the maximum amount of drug released without erosion (∼26%) is closer to the real amount of drug released and the release rates are quite similar. This seems to indicate that erosion is not as crucial in the first phase of drug release in the slow-eroding matrix as it is in study A. Hence, because erosion onset is slow, the amount of drug released during the first 24 h is restricted to drug initially available at the surface and in the external pores of the MS. This is in agreement with the common hypothesis that drug is separated in two different groups, one initially free to diffuse out of the polymer (Batycky et al., 1997; Fu et al., 2003; Huang and Brazel, 2001) and another which needs polymer erosion to be released (Tzafriri, 2000; Liggins and Burt, 2001; Wu et al., 2006).

4.3. Initial drug accessibility: the use of the cellular automaton

Although the idea that drug is separated into two different compartments, one from which it is available for release and one from which it must be freed by erosion, is not new (Tzafriri, 2000; Liggins and Burt, 2001), the use of cellular automaton allows further study of this concept. For example, it is possible to diverge from experimental studies in order to investigate the influence of porosity and drug loading on the initial burst release. Although these aspects were previously studied (Luan et al., 2006; Ravivarapu et al., 2000; Klose et al., 2006; Wu et al., 2006), it is interesting to test, through simulations, different conditions that otherwise could not be obtained experimentally. Accordingly, different simulations were made to measure the initial drug accessibility. The results presented in Fig. 7A show

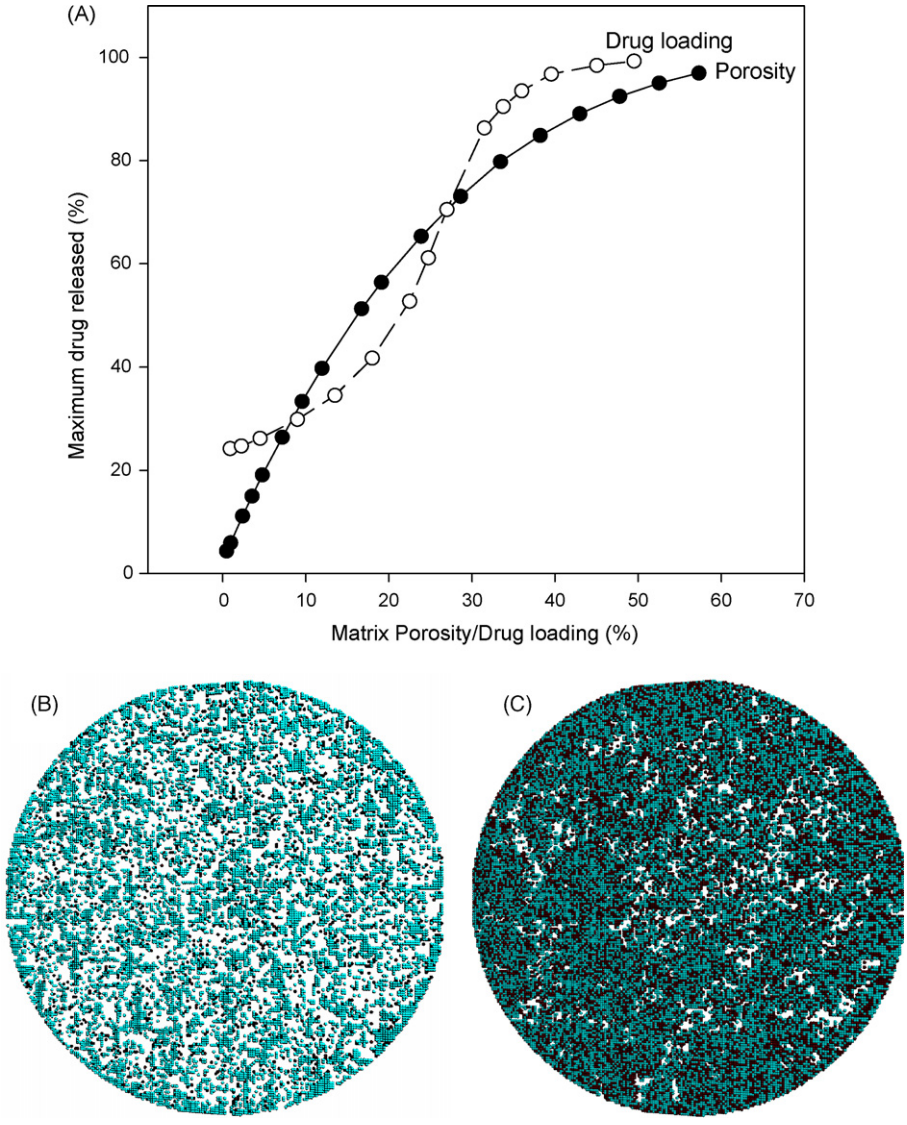

Fig. 7. (A) Maximum drug release for simulations without erosion with different drug loading (◯) and porosities (●). (B) High porosity (60%) leads to high solvent accessibility. (C) High drug loading (45%) leads to high drug clusters connectivity (in black).

maximum drug released without erosion for different matrices with varying porosity (and constant drug loading) or varying drug loading (and constant porosity).

For both parameters, initial accessibility increases with volume occupancy in the matrix. Thus, as expected and in conformity with other experimental observations (Luan et al., 2006; Ravivarapu et al., 2000; Klose et al., 2006), increased pore volume leads to higher solvent penetration throughout the matrix, and thus to higher initial drug release. This is straightforwardly portrayed in Fig. 7B where a longitudinal cut of a matrix with high porosity (60%) show extensive solvent accessibility and pore connectivity.

Likewise, higher drug loading means higher amounts of drug on the surface and it is observed that burst release rates are much faster for higher drug containing matrices (data not shown). However, higher drug amounts on the surface alone cannot explain the sigmoid aspect of the curve. The noticeable accessibility increase in a narrow drug loading range around 20%, previously noticed experimentally (Luan et al., 2006), is typical of percolating systems (Leuenberger et al., 1995; Caraballo et al., 1999; Huang and Brazel, 2001). In these systems, maximum connectivity is reached above a certain threshold (Stauffer and Aharony, 1992). It is thus believed that connectivity of drug clusters might be an important aspect regulating initial accessibility. Once more, Fig. 7C shows a cut from a matrix with high drug loading (45%) where high connectivity between drug clusters leads to extensive drug release (>90%) without any polymer erosion.

Evidently, because an extensive number of parameters might influence experimental accessibility of drug in MS formulations, it is clear that the insights given here only offer a simplistic analysis of the phenomenon. However, it interestingly depicts the consequences of a number of ideal cases of porosity and drug loading on initial drug release.

5. Conclusion

The cellular automaton presented here was shown to provide good correlations with drug release profiles obtained from experimental data, throughout release studies for a specific batch of MS. Initial results seem to offer fairly good representation of phenomena involved in the drug release process; erosion and diffusion. Interestingly, while this simple model gave fairly good correlations with release study A (where polymer degradation occurs rapidly), it is evident that its predictability diminishes in more physiological conditions (where degradation is slower). For these reasons, future works will focus on erosion-specific modifications to better describe the phenomenon, both in fast and slow eroding matrices. Although the exact model design remains unclear, it is thought that putting P cells in relation with each other might efficiently separate degradation from polymer diffusion and tackle relations between molecular weight and erosion.

Alternatively, the cellular automaton was proven to be an interesting way of modeling microspheres in their specific environment. In this work, focus was drawn on drug accessibility attributed to drug loading and porosity. For clarity reasons, both pore and drug cells were distributed according to the method used for previous simulations. However, the model could easily be used to assess influence of other variables on the same parameter (pore size, drug cluster shape or water ingress in the polymer matrix, for example). Likewise, by supplementing conventional models with graphical representations, the cellular automaton will also allow understanding of other important parameters involved in further steps of drug release. For example, simulations with different pore configurations or different drug distributions could provide further comprehension of complex phenomena.

As simulation parameters can be chosen and modified easily, it is believed that cellular automaton's power and descriptivity are limited only by its user's imagination and our understanding of principles involved. Therefore, the presented model is an interesting appendage to the modeling tools already available because it seeks to further extend comprehension of systems while offering fairly good correlations with experiments.

Acknowledgements

The authors would like to thank Mrs. Anda Vintiloiu for helpful advice on writing and correcting the text, and Mr. Jean-Michel Rabanel for critical reviewing of the manuscript.

References

Batycky, R.P., Hanes, J., Langer, R., Edwards, D.A., 1997. A theoretical model of erosion and macromolecular drug release from biodegradable microspheres. J. Pharm. Sci. 86, 1464–1477.

Blanco, D.M., Sastre, R.L., Teijon, C., Olmo, R., Teijon, J.M., 2006. Degradation behaviour of microspheres prepared by spray-drying poly(D,L-lactide) and poly(D,L-lactide-co-glycolide) polymers. Int. J. Pharm. 326, 139–147.

Caraballo, I., Melgoza, J.M., Alvarez-Fuentes, J., Soriano, M.C., Rabasco, A.M., 1999. Design of controlled release inert matrices of naltrexone hydrochloride based on percolation concepts. Int. J. Pharm. 181, 23–30.

Cui, F., Yang, M., Jiang, Y., Cun, D., Lin, W., Fan, Y., Kawashima, Y., 2003. Design of sustained-release nitrendipine microspheres having solid dispersion structure by quasi-emulsion solvent diffusion method. J. Control. Release 91, 375–384.

Delgado, A., Evora, C., Llabres, M., 1996. Degradation of DL-PLA-methadone microspheres during in vitro release. Int. J. Pharm. 140, 219–227.

Dollimore, D., 1964. Improved method for calculation of pore size distribution from adsorption data. J. Appl. Chem. USSR 14, 109.

Dollimore, D., Heal, G.R., 1970. Pore-size distribution in typical adsorbent systems. J. Colloids Interface Sci. 33, 508–519.

Dunne, M., Corrigan, O.I., Ramtoola, Z., 2000. Influence of particle size and dissolution conditions on the degradation properties of polylactide-co-glycolide particles. Biomaterials 21, 1659–1668.

Faisant, N., Siepmann, J., Benoit, J.-P., 2002. PLGA-based microparticles: elucidation of mechanisms and a new, simple mathematical model quantifying drug release. Eur. J. Pharm. Sci. 15, 355–366.

Faisant, N., Siepmann, J., Richard, J., Benoit, J.-P., 2003. Mathematical modeling of drug release from bioerodible microparticles: effect of gamma-irradiation. Eur. J. Pharm. Biopharm. 56, 271–279.

Fu, K., Harrell, R., Zinsky, K., Um, C., Jaklenec, A., Frazier, J., Lotan, N., Burke, P., Klibanov, A.M., Langer, R., 2003. A potential approach for decreasing the burst effect of protein from PLGA microspheres. J. Pharm. Sci. 92, 1582–1591.

Göpferich, A., 1996. Mechanisms of polymer degradation and erosion. Biomaterials 17, 103–114.

Göpferich, A., 1997. Polymer bulk erosion. Macromolecules 30, 2598–2604.

Göpferich, A., Langer, R., 1993. Modeling polymer erosion. Macromolecules 26, 4105–4112.

Göpferich, A., Langer, R., 1995a. Modeling monomer release from bioerodible polymers. J. Control. Release 33, 55–69.

Göpferich, A., Langer, R., 1995b. Modeling of polymer erosion in three dimensions: rotationally symmetric devices. AIChE J. 41, 2292–2299.

Higgins, J.D., Gilmor, T.P., Martellucci, S.A., Bruce, R.D., Brittain, H.G., 2001. Ibuprofen. In: Brittain, H.G. (Ed.), Analytical Profiles of Drug Substances and Excipients, 1st ed. Academic Press, San Diego.

Higuchi, T., 1963. Mechanism of sustained action medication: theoretical analysis of rate of solid drugs dispersed in solid matrices. J. Pharm. Sci. 52, 1145–1149.

Huang, X., Brazel, C.S., 2001. On the importance and mechanisms of burst release in matrix-controlled drug delivery systems. J. Control. Release 73, 121–136.

Kannan, K., Haddad, S., Pelekis, M., 1995. A simple index for representing the discrepancy between simulations of physiological pharmacokinetics models and experimental data. Toxicol. Ind. Health 11, 413–421.

Klose, D., Siepmann, F., Elkharraz, K., Krenzlin, S., Siepmann, J., 2006. How porosity and size affect the drug release mechanisms from PLGA-based microparticles. Int. J. Pharm. 314, 198–206.

Larobina, D., Mensitieri, G., Kipper, M.J., Narasimhan, B., 2002. Mechanistic understanding of degradation in bioerodible polymers for drug delivery. AIChE J. 48, 2960–2970.

Lemaire, V., Belair, J., Hildgen, P., 2003. Structural modeling of drug release from biodegradable porous matrices based on a combined diffusion/erosion process. Int. J. Pharm. 258, 95–107.

Leuenberger, H., Bonny, J.D., Kolb, M., 1995. Percolation effects in matrix-type controlled drug release systems. Int. J. Pharm. 115, 215–224.

Liggins, R.T., Burt, H.M., 2001. Paclitaxel loaded poly(L-lactic acid) microspheres: properties of microspheres made with low molecular weight polymers. Int. J. Pharm. 222, 19–33.

Liggins, R.T., Burt, H.M., 2004. Paclitaxel-loaded poly(L-lactic acid) microspheres 3: blending low and high molecular weight polymers to control morphology and drug release. Int. J. Pharm. 282, 61–71.

Lin, S.Y., Chen, K.S., Teng, H.H., 1999. Protective colloids and polylactic acid coaffecting the polymorphic crystal forms and crystallinity of indomethacin encapsulated in microspheres. J. Microencapsul. 16, 769–776.

Luan, X., Skupin, M., Siepmann, J., Bodmeier, R., 2006. Key parameters affecting the initial release (burst) and encapsulation efficiency of peptide-containing poly(lactide-co-glycolide) microparticles. Int. J. Pharm. 324, 168–175.

Messaritaki, A., Black, S.J., Van Der Walle, C.F., Rigby, S.P., 2005. NMR and confocal microscopy studies of the mechanisms of burst release from PLGA microspheres. J. Control. Release 108, 271–281.

Nadeau, V., Hildgen, P., 2005. AFM study of a new carrier based on PLA and Salen copolymers for gene therapy. Molecules 10, 105–113.

Von Neumann, J., 1966. Theory of Self-reproducing Automata. University of Illinois Press, Urbana, London.

Panoyan, A., Quesnel, R., Hildgen, P., 2003. Injectable nanospheres from a novel multiblock copolymer: cytocompatibility, degradation and *in vitro* release studies. J. Microencapsul. 20, 745–758.

Park, T.G., 1994. Degradation of poly(D,L-lactic acid) microspheres: effect of molecular weight. J. Control. Release 30, 161–173.

Ravivarapu, H.B., Lee, H., Deluca, P.P., 2000. Enhancing initial release of peptide from poly(D,L-lactide-co-glycolide) (PLGA) microspheres by addition of a porosigen and increasing drug load. Pharm. Dev. Technol. 5, 287–296.

Siepmann, J., Faisant, N., Akiki, J., Richard, J., Benoit, J.-P., 2004. Effect of size of biodegradable microparticles on drug release: experiment and theory. J. Control. Release 96, 123–134.

Siepmann, J., Faisant, N., Benoit, J.-P., 2002. A new mathematical model quantifying drug release from bioerodible microparticles using Monte Carlo simulations. Pharm. Res. 19, 1885–1893.

Siepmann, J., Göpferich, A., 2001. Mathematical modeling of bioerodible, polymeric drug delivery systems. Adv. Drug Deliv. Rev. 48, 229–247.

Stauffer, D., Aharony, A., 1992. Introduction to Percolation Theory. Taylor & Francis, London.

Tzafriri, A.R., 2000. Mathematical modeling of diffusion-mediated release from bulk degrading matrices. J. Control. Release 63, 69–79.

Vachon, M.G., Nairn, J.G., 1995. Physicochemical evaluation of Acetylsalicylic Acid-Eudragit(R) RS100 microspheres prepared using a solvent-partition method. J. Microencapsul. 12, 287–305.

Van Drooge, D.J., Hinrichs, W.L.J., Visser, M.R., Frijlink, H.W., 2006. Characterization of the molecular distribution of drugs in glassy solid dispersions at the nano-meter scale, using differential scanning calorimetry and gravimetric water vapour sorption techniques. Int. J. Pharm. 310, 220–229.

Von Burkersroda, F., Schedl, L., Göpferich, A., 2002. Why degradable polymers undergo surface erosion or bulk erosion. Biomaterials 23, 4221–4231.

Wada, R., Hyon, S.-H., Ikada, Y., 1995. Kinetics of diffusion-mediated drug release enhanced by matrix degradation. J. Control. Release 37, 151–160.

Williams, A.C., Timmins, P., Lu, M., Forbes, R.T., 2005. Disorder and dissolution enhancement: deposition of ibuprofen on to insoluble polymers. Eur. J. Pharm. Sci. 26, 288–294.

Wu, X.-G., Li, G., Gao, Y.-L., 2006. Optimization of the preparation of nalfemene-loaded sustained-release microspheres using central composite design. Chem. Pharm. Bull. 54, 977–981.

Zygourakis, K., Markenscoff, P.A., 1996. Computer-aided design of bioerodible devices with optimal release characteristics: a cellular automata approach. Biomaterials 17, 125–135.